

Distributed Frequency-Locked Loops for Wireless Networks

Nicola Varanese*, Osvaldo Simeone[‡], Umberto Spagnolini[†], Yeheskel Bar-Ness[‡]

^{*‡}CWCSPR, New Jersey Institute of Technology,

^{*†}Dipartimento di Elettronica e Informazione, Politecnico di Milano

Email: {nv35, osvaldo.simeone}@njit.edu,
barness@yegal.njit.edu, spagnoli@elet.polimi.it

Abstract—The establishment of a common frequency reference in a distributed wireless network is a critical factor in enabling cooperative communication strategies. In this paper we employ distributed locked loops to entrain the frequencies of autonomous nodes with wireless communication capabilities. Leveraging recent results from the literature on distributed locked loops, the main problem becomes that of designing local frequency difference detectors. After proposing a novel detector, some insight on the dynamical properties of the overall synchronization system are provided and substantiated through the aid of simulation results.

I. INTRODUCTION

The development of decentralized procedures capable of establishing a network-wide time and frequency reference in a wireless network is particularly appealing. As an example, time and frequency synchronization enable cooperative transmissions from multiple nodes without requiring complex receiver structures (see, e.g., [1])¹. Toward this goal, physical layer synchronization protocols are especially attractive due to their features of energy-efficiency, robustness and scalability as compared to packet-level techniques [3].

Until recently, the research activity on distributed synchronization has concentrated on *timing synchronization* [3][4]. Inspired by the pulse-coupling mechanism [3], an efficient protocol for distributed timing synchronization is devised in [4] based on classical work on network synchronization via coupled phase-locked loops [5] and generalizing discrete-time consensus models for networks of agents [6].

In this paper, we focus on the problem of *carrier frequency synchronization* among distributed wireless nodes. It should be noted that, while carrier phase offsets can be easily compensated by the use of non-coherent communication techniques (or other transmission schemes that are insensitive to phase offsets, e.g., Space-Time Coding), frequency offsets - due to local oscillator instabilities or Doppler shifts - are much more deleterious, causing relevant signal distortion. Also, in a wireless environment, where the links between any two nodes introduce different phase shifts, it seems impractical to establish a network-wide phase coherent state, while frequency synchronization appears technologically feasible. Recently, [7] has investigated the problem of estimating and adjusting the

local oscillator frequencies in a two-transmitters-one-receiver system employing Distributed Alamouti STC. The algorithm cannot easily scale to a higher number of nodes and relies on the assignment of specific pilot sequences to each node.

Building mainly on [4] and [6], we propose an algorithm based on distributed frequency-locked loops (DFLL) that is capable to achieve a network-wide frequency synchronous regime for any number of nodes and without any external master reference. We consider a training phase where each node broadcasts a truncated sinusoidal signal with the local carrier frequency. At each node, the local FLL is fed by the output of a frequency difference detector, that extracts from the received signal the weighted sum of the frequency offsets with respect to the other nodes. An approximated analysis of the resulting dynamic system is carried out using tools from the literature on consensus algorithms on random graphs [8][9]. Moreover, numerical results validate our findings.

II. SYSTEM MODEL AND MAIN ASSUMPTIONS

The network we consider is composed of K nodes, where the k -th node's local carrier frequency is f_k . The objective of the network is to reach network-wide frequency synchronization through the exchange of specific waveforms. We assume that the nodes already share a common notion of time, having reached an agreement on a large-scale timing clock (frame synchronization) using one among several feasible algorithms, e.g., [3] [4]. This enables the time axis to be divided into time-slots, or observation intervals, each of duration T_0 seconds. Focusing on a training phase, we assume that, in any n -th slot, each k -th node broadcasts a sequence of band-limited pulses modulating a sinusoid at the current local carrier frequency $f_k[n]$. Namely, the base-band model of the transmitted signal in the n -th period, for t within the observation window T_0 is

$$x_k(t; n) = \sum_{l=0}^{L-1} g(t - \tau_k[n] - lT_s) e^{j(2\pi f_k[n]t + \phi_k[n])}, \quad (1)$$

where $\tau_k[n]$ is a residual timing offset with respect to the ideal reference, $\phi_k[n]$ is the initial carrier phase and $T_s = T_0/L$ is the pulse period. The signal $g(t)$ is assumed to be a Nyquist pulse with bandwidth $1/2T_s$, so that the system RF bandwidth is $1/T_s$. The delay $\tau_k[n]$ and the carrier phase $\phi_k[n]$ are due to residual frame asynchronism and switching delays. In the

¹However, see [2] for an asynchronous approach to simple wireless networks.

following, we assume $\tau_k[n] \ll T_s$ and $f_k[n] \ll 1/T_s$. Notice that the current local frequency $f_k[n]$ is adjusted via the local FLL as discussed below, while the phase $\phi_k[n]$ can be assumed uniformly distributed in $[-\pi, \pi]$.

The wireless channel between any pair of nodes (i, k) is modeled as a time-invariant complex scalar gain $h_{k,i} = |h_{k,i}|e^{j\psi_{k,i}}$, where the energy of the channel is inversely proportional to the geometric distance between the two nodes according to a power law $|h_{k,i}|^2 \propto d_{k,i}^{-\alpha}$. To simplify, we assume that all the nodes transmit with equal power, the channel is reciprocal $h_{k,i} = h_{i,k}$ (due to time division duplexing), and propagation delays are negligible compared to the pulse period T_s .

A. Distributed Frequency Locked Loops (DFLLs)

In this subsection we review the basic principle underlying the DFLLs. In order to focus on the basics, we make the ideal assumption (to be removed in the next sections) that each node is able to calculate the frequency offsets between its local oscillator and the other oscillators in the network. Namely, let $f_i^k[n]$ be the difference between the carrier frequency at the i -th node and the local reference at the k -th node (i.e., $f_i^k[n] = f_i[n] - f_{0,k}$, where $f_{0,k}$ is the local carrier frequency reference), each node k is assumed to be able to compute a weighted sum of frequency offsets

$$\bar{e}_k[n] = \frac{\sum_{i \neq k} a_{k,i} (f_i^k[n] - f_k^k[n])}{\sum_{i \neq k} a_{k,i}} = \frac{e_k[n]}{\sum_{i \neq k} a_{k,i}}, \quad (2)$$

where $a_{k,i}$ are real positive weights depending on the physical characteristics of the directed link connecting the i -th node with the k -th node. Based on the error $\bar{e}_k[n]$, each k -th node can update the local frequency as

$$f_k^k[n+1] = f_k^k[n] + \epsilon \bar{e}_k[n], \quad (3)$$

where $f_k^k[n]$ is the k -th node local frequency offset in the n -th time-slot and ϵ is the step size.

It was shown in [4] that the update rule in (3) can be regarded as a first-order discrete-time locked loop, where, in our case, the locking variable is the frequency $f_i[n]$ (Frequency Locked Loop - FLL), and the input to the loop is a weighted sum of the frequencies employed by the other nodes. The update rule (3) is also an instance of consensus algorithms, see, e.g., [8][6].

It is useful for convergence analysis to interpret (3) with the aid of graph-theoretic tools. Following the lines of [6][4], the network can be modeled as a weighted directed graph $\mathcal{G} = (\mathcal{V}, \mathcal{E}, \mathbf{A})$ of order K , where $\mathcal{V} = 1, \dots, K$ is the set of nodes, $\mathcal{E} \subseteq \mathcal{V} \times \mathcal{V}$ is the set of edges weighted by the off-diagonal elements of the $K \times K$ adjacency matrix $[\mathbf{A}]_{k,i} = a_{k,i}$ ($[\mathbf{A}]_{i,i} = 0$). The *graph Laplacian* \mathbf{L} is defined as $\mathbf{L} = \mathbf{D} - \mathbf{A}$ where $[\mathbf{D}]_{k,k} = d_k$ is the diagonal matrix of the in-degrees $d_k = \sum_{i \neq k} a_{k,i}$. A directed graph is said to be *strongly connected* if there exist a directed path (i.e., a collection of edges in \mathcal{E}) connecting any pair of nodes in the graph. Operating a change of variable $f_i[n] = f_i^k[n] + f_{0,k}$, and defining the vector containing the frequencies of all nodes

as $\mathbf{f}[n] = [f_1[n], \dots, f_K[n]]^T$, we can express (3) compactly as the vector difference equation

$$\mathbf{f}[n+1] = \mathbf{f}[n] - \epsilon \mathbf{D}^{-1} \mathbf{L} \mathbf{f}[n] = \bar{\mathbf{P}}_\epsilon \mathbf{f}[n]. \quad (4)$$

where $\bar{\mathbf{P}}_\epsilon = \mathbf{I} - \epsilon \mathbf{D}^{-1} \mathbf{L}$ is the normalized *Perron* matrix of the graph \mathcal{G} with parameter ϵ . By construction, the matrix $\bar{\mathbf{P}}_\epsilon$ is nonnegative and row stochastic since $\bar{\mathbf{P}}_\epsilon \cdot \mathbf{1} = \mathbf{1}$. By reaching a synchronized state, we mean that all the K nodes converge to the same value $f_1^* = f_2^* = \dots = f_K^* = f^*$. As shown in [6], a synchronization (consensus) point $\mathbf{f}^* = f^* \mathbf{1}$ is globally asymptotically stable for all initial states $\mathbf{f}[0]$ if the directed graph \mathcal{G} is strongly connected and $\epsilon \in (0, 1)$.

In the following, we intend to employ (4) to achieve frequency synchronization in a network of sensors with radio communication capabilities. Differently from the idealized model presented above, the frequency is a parameter embedded in the waveform (1) transmitted by each node. Therefore, a suitable frequency difference detector has to be devised in order to extract the desired error signal $\bar{e}_k[n]$ (2) from the received signal samples.

III. DESIGN OF THE FREQUENCY DIFFERENCE DETECTOR

In this section we address the problem of designing an appropriate frequency difference detector that approximates (2) to realize DFLLs under the assumptions on network and node operation as described above. We further assume that every node can operate with *full duplex* capabilities. This means that during a time-slot each node is both transmitting its own signal while receiving signals from the other nodes². During any time-slot, due to the broadcast nature of the wireless medium, a superposition of all the signals (1) transmitted in the network appears at the input k -th node receiving interface. The received RF signal is down-converted to baseband through the local frequency reference $f_{0,k}$, filtered by matched filter and sampled at frequency $1/T_s$. As a consequence, the sampled received signal at each node k is

$$\tilde{y}_k^F(lT_s; n) = \sum_{i \in \mathcal{A}[n]} h_{k,i}[n] e^{j(2\pi f_i^k[n] l T_s + \tilde{\phi}_{k,i}[n])}, \quad (5)$$

where $f_i^k[n] = f_i[n] - f_{0,k}$ and the phase $\tilde{\phi}_{k,i}[n]$ includes the timing offset $\tau_{k,i}[n]$ (overall due to timing errors and propagation delays). For simplicity, we are neglecting the Additive Gaussian Noise (AGN) at the receiving interface as its impact will be reported elsewhere. For the time being, we refer the reader to the literature for viable general countermeasures to convergence impairments due to AGN [8]. The received signal after demodulation of (5) with $f_k^k[n] = f_k[n] - f_{0,k}$ is

$$y_k^F(lT_s; n) = \sum_{i \in \mathcal{A}[n]} |h_{k,i}[n]| e^{j(2\pi(f_i^k[n] - f_k^k[n]) l T_s + \phi_{k,i}[n])}, \quad (6)$$

²Introducing half-duplex constraints, namely transmit/receive cycles, would lead to a time-varying network topology. While this scenario is outside the scope of this work, we refer the reader to [10] for an analysis of convergence conditions for general coupled dynamical systems.

where $\phi_{k,i}[n] = -2\pi f_i[n]\tau_{k,i}[n] + \psi_{k,i} + (\phi_i[n] - \phi_k[n])$ is the overall phase offset between the i -th and the k -th node. It is important to remark here that, due to the different contributions, the phase $\phi_{k,i}[n]$ is neither reciprocal ($\phi_{k,i}[n] \neq \phi_{i,k}[n]$), nor symmetric ($\phi_{k,i}[n] \neq -\phi_{i,k}[n]$). Overall due to the uniform distribution of $\phi_i[n]$, $\phi_{k,i}[n]$ is also uniform on $[-\pi, \pi]$, and independent of $f_i[n]$.

The signal in (6) is the input of the frequency difference detector, which has to extract the desired error signal (2). To allow useful approximations, let $T_0 \rightarrow \infty$ so that setting $a_{k,i} = |h_{k,i}|^2$, and recalling (6), it can be shown that

$$e_k[n] = \sum_{i \neq k} a_{k,i} (f_i[n] - f_k[n]) = \int_{-\infty}^{\infty} f \cdot |Y_k(f; n)|^2 df, \quad (7)$$

and

$$\bar{e}_k[n] = \frac{e_k[n]}{\sum_{i \neq k} a_{k,i}} = \frac{\int_{-\infty}^{\infty} f \cdot |Y_k(f; n)|^2 df}{\int_{-\infty}^{\infty} |Y_k(f; n)|^2 df}, \quad (8)$$

where $|Y_k(f; n)|^2$ is the energy spectrum of the received signal $y_k(lT_s; n)$ (6). As shown in the Appendix, for a sampling interval T_s and L odd ($L \geq 3$), the error (7)-(8) becomes

$$e_k[n] \simeq \frac{1}{2\pi} \text{Im} \left\{ \sum_{m=0}^{\frac{L-3}{2}} y_k((2m+2)T_s; n) y_k^*((2m+1)T_s; n) + y_k(2mT_s; n) y_k^*((2m+1)T_s; n) \right\}, \quad (9)$$

$$\bar{e}_k[n] \simeq \frac{e_k[n]}{2T_s \sum_{m=0}^{\frac{L-3}{2}} |y_k((2m+1)T_s; n)|^2}. \quad (10)$$

Both (7) and (8) could be also evaluated using DFT-based spectral methods. In Sec. V, the performance of (10) is compared to a detector based on the FFT of the L samples of the received signal $y_k(lT_s, n)$.

IV. DISCUSSION ON THE CONVERGENCE OF THE PROPOSED ALGORITHM

Given the signal model in (6) and the frequency difference detectors in (9) and (10), in this section we study the properties of the resulting dynamical system of DFLLs that approximates (4). By plugging (6) in (9), after tedious algebraic computations, it can be shown that the error signal (9) reads

$$e_k \simeq \frac{L}{\pi} \sum_{i \neq k} w_{k,i} \sin(2\pi(f_i^k - f_k^k)T_s), \quad (11)$$

where the real valued weights

$$w_{k,i} = |h_{k,i}|^2 + v_{k,i}, \quad (12)$$

are random variables with a random coupling term

$$v_{k,i} = \frac{|h_{k,i}|}{L} \times \sum_{l \neq k, i} |h_{k,l}| \sum_{m=0}^{\frac{L-3}{2}} \cos(2\pi(f_i^k - f_l^k)(2m+1)T_s + \phi_{k,i} - \phi_{k,l}). \quad (13)$$

Notice that we have neglected the dependency on the iteration index n in order to simplify the notation. In order to derive the output of the normalized detector (10), we divide (11) by $\sum_{i \neq k} a_{k,i}$ approximated in (22). It can be shown that

$$\sum_{i \neq k} a_{k,i} \simeq 2T_s \sum_{m=0}^{\frac{L-3}{2}} |y_k((2m+1)T_s; n)|^2 = 2LT_s \sum_{i \neq k} (|h_{k,i}|^2 + v_{k,i}) = 2LT_s \sum_{i \neq k} w_{k,i}, \quad (14)$$

thus yielding the normalized output

$$\bar{e}_k \simeq \frac{1}{2\pi T_s} \frac{\sum_{i \neq k} w_{k,i} \sin(2\pi(f_i^k - f_k^k)T_s)}{\sum_{i \neq k} w_{k,i}}. \quad (15)$$

Each normalized weight $w_{k,i} / \sum_{i \neq k} w_{k,i}$ is a non-linear combination of the $w_{k,i}$ and is in general non-zero mean. From (11), we can see that the devised detector (9) (and (10)) has a nonlinear sinusoidal characteristic, as a consequence of the discretization of the differential operator that led to the approximation (9)-(10) (see the Appendix for details). Increasing the sample rate $1/T_s$ (or equivalently the system bandwidth) would linearize the characteristic. Further, it should be noted that if we let the number of available samples within the observation interval $L \rightarrow \infty$, the coupling term $v_{k,i}$ in (12) tends to zero and we have perfect decoupling of the contributions from different nodes, each weighted by the modulus of their respective channel, as in the ideal detector (2). In the following, we further study the above mentioned cases of large bandwidth and large observation window T_0 . For a finite L , the coupling $v_{k,i}$ depends on the random phases $\phi_{k,i}$. In particular, the coefficients $v_{k,i}$ are in general zero-mean correlated random variables.

Large bandwidth and $L = 3$: Assume $L = 3$ and $f_i[n] \ll 1/T_s$, so as to linearize the error signal (15) and thus obtain that the linear dynamical system of DFLLs (3) reduces to

$$f_k^k[n+1] = f_k^k[n] + \epsilon \frac{\sum_{i \neq k} w_{k,i}[n] (f_i^k[n] - f_k^k[n])}{\sum_{i \neq k} w_{k,i}[n]}, \quad (16)$$

where the distribution of $w_{k,i}[n]$ depends only on the random phases $\phi_{k,i}[n]$. Equation (16) can be cast into vector form analogously to (4) as

$$\mathbf{f}[n+1] = \mathbf{f}[n] - \epsilon \mathbf{D}^{-1}[n] \mathbf{L}[n] \mathbf{f}[n] = \bar{\mathbf{P}}_\epsilon[n] \mathbf{f}[n], \quad (17)$$

where we emphasized the dependency of $\bar{\mathbf{P}}$ from the loop gain ϵ . From (12), it is easy to see that $\mathbf{L}[n] = \mathbf{L} + \mathbf{L}_v[n]$, $\mathbf{D}[n] = \mathbf{D} + \mathbf{D}_v[n]$, where $\mathbf{L}_v[n]$ and $\mathbf{D}_v[n]$ depend linearly on the $v_{k,i}$, and are therefore random matrices with zero-mean

entries. The nonlinear dependence of the system matrix $\bar{\mathbf{P}}_\epsilon[n]$ on the weights $w_{k,i}$ does not allow us to make any assumption on its distribution. We can only say that $\bar{\mathbf{P}}_\epsilon[n]$ and $\bar{\mathbf{P}}_\epsilon[m]$ are independent and identically distributed for $n \neq m$. The system in (17) is a stochastic Linear Time Variant dynamical system (or linear system with multiplicative noise), which is quite well-studied in the literature on stochastic control theory.

Let the $(K-1) \times K$ matrix \mathbf{Q} be such that $\mathbf{Q}^T \mathbf{1} = \mathbf{0}$ and $\mathbf{Q}^T \mathbf{Q} = \mathbf{I}_{K-1}$. It was shown in [11] [9] that a sufficient condition for almost sure (i.e., with probability 1) synchronization is that the eigenvalues of the matrix

$$\mathbf{\Pi}_\epsilon = E[\tilde{\mathbf{P}}_\epsilon^T[n] \otimes \tilde{\mathbf{P}}_\epsilon^T[n]] \quad (18)$$

be inside the unit circle, where $\tilde{\mathbf{P}}_\epsilon[n] = \mathbf{Q}^T \bar{\mathbf{P}}_\epsilon[n] \mathbf{Q}$ and \otimes denotes the Kronecker product. Therefore, the maximum admissible value of the loop gain for which the system reaches consensus w.p.1 is the smallest ϵ that forces the eigenvalues of $\mathbf{\Pi}_\epsilon$ to leave the open unit circle. It is interesting to note how, in the case of a deterministic system matrix $\bar{\mathbf{P}}_\epsilon$, this requirement corresponds to the well known constraint on the subdominant eigenvalue of the system matrix $\lambda_2(\bar{\mathbf{P}}_\epsilon) < 1$ [6].

Large observation window: Assume $L \rightarrow \infty$ ($T_0 \rightarrow \infty$), we are left with a deterministic nonlinear dynamical system of the form

$$f_k^k[n+1] = f_k^k[n] + \frac{1}{2\pi T_s} \frac{\sum_{i \neq k} |h_{k,i}|^2 \sin(2\pi(f_i^k[n] - f_k^k[n])T_s)}{\sum_{i \neq k} |h_{k,i}|^2}. \quad (19)$$

The periodicity of the detector response could cause dangerous aliasing effects, possibly letting a node lock on a frequency that is outside the system bandwidth (*false lock* event). A convergence analysis of a system analogous to (19) was carried out in [12], where it was noticed that, for an all-to-all connection topology, a sufficient condition to avoid false locks is $f_i^k[0] \in (\gamma - 1/4T_s, \gamma + 1/4T_s)$ where γ is an arbitrary constant. This leads us to conclude that, in a general topology with finite L , the proposed detector could be employed for fine frequency tuning only when $f_i^k[0] \ll 1/T_s$.

V. NUMERICAL SIMULATIONS

In this section we validate the discussion in Sec. IV for a system where $K = 4$ nodes are grouped in two clusters as in Fig. 1. The channels are fixed complex scalars with amplitude

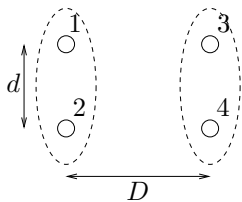


Fig. 1. The simple topology considered in Sec. V.

$|h_{k,i}| = d_{k,i}^{-3/2}$. The starting point is always assumed to be $\mathbf{f}[0] = f_0 + [0.15, 0.05, -0.05, -0.15]^T/T_s$, where f_0 is

the nominal carrier frequency of the communication system.. In this setting, for the deterministic system (19) (that is for $L \rightarrow \infty$) there is no possible occurrence of false locks. Due to the random nature of the connections, for finite L false locks do occur but with a rapidly decreasing probability as L grows. For the sake of clarity, the following simulation results do not include the cases where a false lock occurs. We will compare the proposed algorithm with a FFT-based algorithm, which estimates the first moment of the power spectrum of the received signal through the FFT of the L samples available.

In Fig. 2 we show the mean deviation $\sqrt{E[\xi^2[n]]}$ of the frequency vector $\mathbf{f}[n]$ versus n for different values of

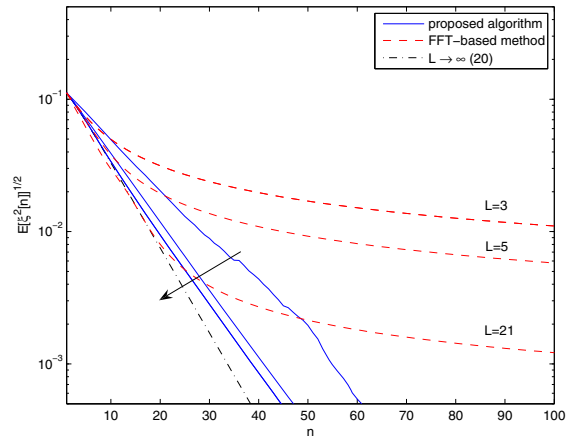


Fig. 2. Mean deviation of the frequency vector $\mathbf{f}[n]$ for different algorithms ($D/d = 1.2$, $\epsilon = 0.15$, $L = 3, 5, 21$).

$L = 3, 5, 21$, where $E[\xi^2[n]] = 1/4E[\sum_{k=1}^4 (f_k[n] - 1/4 \sum_{k=1}^4 f_k[n])^2]$, and the expectation is taken over different runs of the algorithm. In this case $D/d = 1.2$, $\epsilon = 0.15$, and for $L = 3$ the eigenvalues of the matrix $\mathbf{\Pi}_\epsilon$ can be shown by numerical results to be all inside the unit circle. Indeed, the nonlinear system is able to achieve consensus w.p.1 for all the values of L , greater L simply improving convergence speed. As far as the occurrence of false lock events, with $L = 3$ the probability of a false lock is 0.0148, and is already zero for $L = 5$. The FFT-based algorithm is inevitably limited by the few frequency samples available. Despite an intrinsic resilience to false locks, the convergence speed of this algorithm dramatically reduces after few iterations, and it can achieve synchronization only to a finite precision for a practical number of iterations.

Finally, in Fig. 3 we show how the use of $L > 3$ is beneficial in order to control the behavior of the proposed synchronization algorithm. In particular we consider the case $D/d = 2$ and $\epsilon = 0.35$, where for $L = 3$ the eigenvalues of $\mathbf{\Pi}_\epsilon$ do not lie all inside the unit circle. From Fig. 3 it is seen that for $L = 3$ the algorithm is not able to approach a sufficient degree of synchronization, and the probability of false locks is also intolerably high in this case. Indeed, for any value $L > 3$ the proposed algorithm achieves a lower

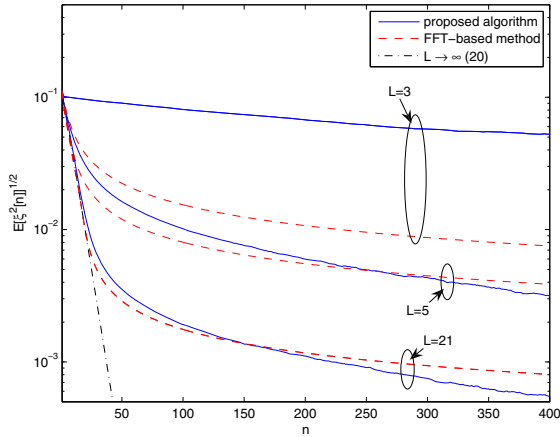


Fig. 3. Mean deviation of the frequency vector $\mathbf{f}[n]$ for different algorithms ($D/d = 2$, $\epsilon = 0.35$, $L = 3, 5, 21$).

mean deviation as compared to the FFT-based method³ with practically no occurrences of false locks.

VI. CONCLUSIONS

In this work, coupled discrete-time locked loops have been investigated as means to attain frequency synchronization within an ensemble of nodes with wireless communication capabilities. Specifically, a novel frequency detector has been designed for this purpose, with a lower complexity as compared to FFT-based solutions. The convergence properties of the resulting dynamical system have been studied with the aid of known results from control theory and computer simulations. Numerical results show that, when the nodes in the network are close to each other, the proposed algorithm is capable of achieving synchronization already with three samples per observation interval. On the other hand, a larger number of time samples allows robust frequency synchronization under general network conditions.

APPENDIX

The normalized error (8) can be approximated via an estimate of the first-order moment of the power spectral density $|Y_k(f; n)|^2$. Based on this idea, here we derive the approximations (10) and (9), by adapting the treatment in [13]. Let us start considering the error signal in (7). By recalling that $|Y_k(f; n)|^2$ is the Fourier transform of the deterministic autocorrelation of the received signal $r_{y_k}(t; n) = \int_{-\infty}^{+\infty} y_k(t + \tau; n) y_k^*(\tau; n) d\tau$, it is possible to write (7) in the time domain as $e_k[n] = \frac{1}{2\pi j} \int_{-\infty}^{+\infty} j2\pi f |Y_k(f; n)|^2 df = \frac{1}{2\pi j} \left. \frac{dr_{y_k}(t; n)}{dt} \right|_{t=0}$. Since we are looking for a sampled detector, we approximate the continuous-time autocorrelation with the autocorrelation of the *sampled* input $\tilde{r}_{y_k}(mT_s; n) = T_s y_k(mT_s; n) * y_k^*(-mT_s; n)$. By employing a first-order finite

³It should be noted how the proposed algorithm has a computational complexity only linear in L , while the FFT algorithm requires $O(L \log L)$ multiplications.

difference in lieu of the derivative, (7) can be approximated by

$$e_k[n] \simeq \frac{1}{2\pi j} \frac{\tilde{r}_{y_k}(T_s; n) - \tilde{r}_{y_k}(-T_s; n)}{2T_s}, \quad (20)$$

By expliciting the autocorrelation in (20), for L odd it can be shown that the detector (7) is approximated by

$$e_k[n] \simeq \frac{1}{2\pi} \text{Im} \left\{ \sum_{m=-\infty}^{+\infty} y_k((2m+2)T_s; n) y_k^*((2m+1)T_s; n) - y_k(2mT_s; n) y_k^*((2m+1)T_s; n) \right\}. \quad (21)$$

Since we intend to use the normalized error signal $\bar{e}_k[n] = e_k[n] / \sum_{i \neq k} a_{k,i}$, it is also easy to see that

$$\sum_{i \neq k} a_{k,i} \simeq 2T_s \sum_{m=-\infty}^{+\infty} |y_k((2m+1)T_s; n)|^2, \quad (22)$$

following the footsteps of the previous treatment. Here a sampling period $2T_s$ was used in order to simplify the detector.

Finally, in both cases, we have to account for a finite observation interval $T_0 = LT_s$, thus limiting all the summations on a finite range of values, yielding the desired result in (9) and (10).

REFERENCES

- [1] G. Kramer, I. Maric, and R. D. Yates, *Cooperative communications*. Now Publishers, 2007.
- [2] D. Petrovic, K. Ramchandran, and J. Rabaey, "Overcoming untuned radios in wireless networks with network coding," *IEEE Trans. Inform. Theory*, vol. 52, pp. 2649–2657, June 2006.
- [3] Y. W. Hong and A. Scaglione, "A scalable synchronization protocol for large scale sensor networks and its applications," *IEEE J. Select. Areas Commun.*, vol. 23, p. 10851099, May 2005.
- [4] O. Simeone and U. Spagnolini, "Distributed synchronization for wireless sensor networks with couple discrete-time oscillators," in *Eurasip Journal on Wireless Commun. and Networking*, vol. 2007, July 2007, pp. 3153–3167.
- [5] W. C. Lindsey, F. Ghazvinian, W. C. Hagmann, and K. Dessouky, "Network synchronization," *Proc. IEEE*, vol. 73, pp. 1445–1467, Oct. 1985.
- [6] R. Olfati-Saber and R. M. Murray, "Consensus problems in networks of agents with switching topology and time-delays," *IEEE Trans. Automat. Contr.*, vol. 49, pp. 1520–1533, Sept. 2004.
- [7] P. Parker, P. Mitran, D. W. Bliss, and V. Tarokh, "On bounds and algorithms for frequency synchronization for collaborative communication systems." [Online]. Available: http://arxiv.org/PS_cache/arxiv/pdf/0704/0704.3054v1.pdf
- [8] S. Kar and J. M. F. Moura, "Distributed consensus algorithms in sensor networks: Link failures and channel noise." [Online]. Available: http://arxiv.org/PS_cache/arxiv/pdf/0711/0711.3915v1.pdf
- [9] M. Porfiri, "Consensus seeking over random weighted directed graphs," *IEEE Trans. Automat. Contr.*, vol. 52, pp. 1767–1773, Sept. 2007.
- [10] L. Moreau, "Stability of multiagent systems with time-dependent communication links," *IEEE Trans. Automat. Contr.*, vol. 50, pp. 169–182, Feb. 2005.
- [11] H. J. Kushner, *Introduction to stochastic control*. Holt, Rinehart and Winston, 1971.
- [12] B. I. Triplett, D. J. Klein, and K. A. Morgansen, "Discrete time Kuramoto models with delay," in *Workshop on Networked Embedded Sensing and Control*, vol. 2005, Oct. 2005.
- [13] K. Miller and M. Rochwarger, "A covariance approach to spectral moment estimation," *IEEE Trans. Inform. Theory*, vol. 5, pp. 588–596, Sept. 1972.